

# Geometry-induced modification of fluctuation spectrum in quasi-two-dimensional condensates

Arko Roy<sup>1,2,†</sup> and D. Angom<sup>1,§</sup>

<sup>1</sup>Physical Research Laboratory, Navrangpura, Ahmedabad-380009, Gujarat, India

<sup>2</sup>Indian Institute of Technology, Gandhinagar, Ahmedabad-382424, Gujarat, India

E-mail: [angom@prl.res.in](mailto:angom@prl.res.in)

**Abstract.** We report the structural transformation of the low-lying spectral modes, especially the Kohn mode, from radial to circular topology as harmonic confining potential is modified to a toroidal one, and this corresponds to a transition from simply to multiply connected geometry. For this we employ the Hartree-Fock-Bogoliubov theory to examine the evolution of low energy quasiparticles. We, then, use the Hartree-Fock-Bogoliubov theory with the Popov approximation to demonstrate the two striking features of quantum and thermal fluctuations. At  $T = 0$ , the non-condensate density due to interaction induced quantum fluctuations increases with the transformation from pancake to toroidal geometry. The other feature is, there is a marked change in the density profile of the non-condensate density at finite temperatures with the modification of trapping potential. In particular, the condensate and non-condensate density distributions have overlapping maxima in the toroidal condensate, which is in stark contrast to the case of pancake geometry. The genesis of this difference lies in the nature of the thermal fluctuations.

*Keywords:* Bose-Einstein condensates, Toroidal Bose-Einstein condensates, collective excitations, finite temperature effects

† Corresponding author: [arkoroy@prl.res.in](mailto:arkoroy@prl.res.in)

§ Corresponding author: [angom@prl.res.in](mailto:angom@prl.res.in)

## 1. Introduction

Topological defects are generated spontaneously during phase transitions, and Bose-Einstein condensation is no exception. One approach to understand the seeding of the topological defects is through the Kibble-Zurek (KZ) mechanism [1, 2]. In recent times, the realization of Bose-Einstein condensates (BECs) in multiply connected (toroidal) geometries [3–6] have opened up new vistas to examine this mechanism in detail. Here, one may ask “What is the basic nature of the fluctuations in toroidal condensates ?” Answer to this question can provide fundamental understanding on the scale, structure, and energetics of the defect formation. It is well known that dimensionality, and fluctuations play a major role in the formation of BECs. In brief, a three-dimensional (3D) Bose gas can undergo a phase transition to a BEC at non-zero temperatures. However, following the Mermin-Wagner-Hohenberg theorem [7–9], thermal fluctuations restrict the transition to BEC for a two-dimensional (2D) Bose gas. The 2D Bose gases instead undergo a Berezinskii-Kosterlitz-Thouless (BKT) [10–12] transition to a quasicohesent superfluid state [13–15], and similar transition occurs in quasi-2D Bose systems [14–19]. The BKT transition is relevant to the simply connected geometry (pancake) of the system under consideration in the present work. We, however, focus our attention to the toroidal geometry as the effects of thermal fluctuations in KZ mechanism is our main interest, and use the pancake geometry as the initial state for comparison.

Apart from phase transitions, topological defects are also created in fluid flows as well. In BECs, the velocity of pointlike defects, which must exceed a critical value, plays a vital role in the nucleation of topological defects like vortices. In simply connected BECs the critical velocity to create excitations due to a pointlike defect or a non-stationary obstacle has been experimentally measured [20–23], and similar study with toroidal BECs were reported in a recent experimental work [24]. Furthermore, persistence and decay of superfluid flow in toroidal BECs have been observed in experiments through the appearance of vortex-antivortex pairs [4] in the presence of an obstacle exceeding a critical velocity.

To gain insights on the quantum, and thermal fluctuations in toroidal condensates vis-a-vis pancake shaped condensates, we examine the quasiparticle spectrum as the confining potential is modified from harmonic to a Mexican hat potential. We demonstrate, using the Hartree-Fock-Bogoliubov theory, novel features in the evolution of the low-energy quasiparticle amplitudes. For example, our studies reveal that the energy of the Kohn mode, namely sloshing mode, decreases on steering simply connected or pancake shaped condensate to multiply connected or toroidal condensate. This is attributed to the fact that in the latter, the predominant excitations are along the axis of the toroid. Hence, the effective wavenumber of the Kohn mode is lower than in pancake geometry. Furthermore at  $T \neq 0$  when the condensate is multiply connected, the maxima of the condensate and the thermal densities tend to coincide. This, however, is not the case in simply connected condensates. Experimentally, it is possible to

transform harmonic to toroidal traps [25], by combining a harmonic potential with a Gaussian potential. This is the scheme we have adopted in the present work. Toroidal confining potential, however, can also be realized with Laguerre-Gaussian ( $\text{LG}_p^l$ ) laser beams, and were first examined in theoretical works [26, 27]. Here,  $p \geq 0$  and  $l$ , are radial and azimuthal orders of the laser beam, respectively. Following which, toroidal condensates of atomic  $^{23}\text{Na}$  [4], and  $^{87}\text{Rb}$  [5] have been achieved using  $\text{LG}_0^l$  beams [28]. Furthermore, toroidal trapping potentials for  $^{87}\text{Rb}$  condensates have been realized by combining an RF-dressed magnetic trap with an optical potential [3] or by the intersection of three light beams as elucidated in Ref. [6]. Our present investigation has profound experimental implications since, the more commonly used approach to produce toroidal traps using  $\text{LG}_p^l$  laser beams do not have limiting case equivalent to a harmonic oscillator potential. For this reason,  $\text{LG}_p^l$  laser beams are not suitable to examine the variation in fluctuations as a pancake shaped condensate is transformed to a toroidal one.

As mentioned earlier, the role of fluctuations in the generation of topological defects in toroidal BECs demands a good understanding of the quasiparticle modes. To this end, we employ the gapless Hartree-Fock-Bogoliubov theory with the Popov approximation (HFB-Popov) to compute the energy eigenspectra of the quasiparticle excitations of these condensates and demonstrate its distinct features.

The remaining of the paper consists of Sec. 2, which provides a brief explanation of the HFB-Popov formalism for interacting quasi-2D BEC to compute the quantum and thermal fluctuations. In the same section, we also provide a description of the Stochastic Gross-Pitavetskii (SGP) approach to incorporate thermal fluctuations in BECs. The results and discussions are given in Sec. 3. In this section the evolution of the Bogoliubov quasiparticle energies and amplitudes based on present studies are presented. We also highlight the change in the structure of quantum and thermal fluctuations due to the change in the geometry of the external confining potential. Finally, we end with conclusions highlighting the key findings of the present work in Sec. 4.

## 2. Theoretical methods

In a quasi-2D trapped BEC, the trapping frequencies of the harmonic oscillator potential  $V(x, y, z) = (1/2)m\omega_x^2(x^2 + \alpha^2 y^2 + \lambda^2 z^2)$  satisfy the condition  $\omega_x, \omega_y \ll \omega_z$ , and  $\hbar\omega_z \gg \mu$ . Here,  $\alpha = \omega_y/\omega_x$  and  $\lambda = \omega_z/\omega_x$  are the anisotropy parameters along the transverse and axial directions, respectively. For  $\lambda \gg 1$  and  $\alpha = 1$  or quasi-2D BEC, the axial degrees of freedom can be integrated out and only the transverse excitations contribute to the dynamics. Under the mean field approximation, in Cartesian coordinate system, the second quantized form of the grand-canonical Hamiltonian of the system is

$$\hat{H} = \iint dxdy \hat{\Psi}^\dagger(x, y, t) \left[ -\frac{\hbar^2}{2m} \nabla_\perp^2 + V(x, y) - \mu + \frac{U}{2} \hat{\Psi}^\dagger(x, y, t) \hat{\Psi}(x, y, t) \right] \hat{\Psi}(x, y, t). \quad (1)$$

Here,  $\hat{\Psi}$  and  $\mu$  are the Bose field operator with BEC, and the chemical potential, respectively with  $\nabla_\perp^2 = \partial^2/\partial x^2 + \partial^2/\partial y^2$ . The inter-atomic interaction  $U = 2a\sqrt{2\pi\lambda}$

, where  $a > 0$  is the  $s$ -wave scattering length, and  $m$  is the atomic mass. In the present work, to examine toroidal condensates vis-a-vis pancake shaped condensates, we superimpose a 2D-Gaussian potential to the harmonic oscillator potential. The confining potential is thus  $V_{\text{net}}(x, y) = V(x, y) + U_0 e^{-(x^2 + \alpha^2 y^2)/2\sigma^2}$  with  $U_0$  and  $\sigma$  as the strength and radial width of the Gaussian potential, respectively. With  $\alpha = 1$ ,  $V_{\text{net}}$  is rotationally symmetric, the symmetry is, however, broken when  $\alpha < 1$ . The equipotential curves are then ellipses with semi-major axis along  $y$ -axis. Furthermore, when  $U_0 \gg 0$ ,  $V_{\text{net}}$  is modified, and at higher values of  $U_0$  the potential assumes the form of a doughnut or a toroid. Thus tuning  $U_0$ , we can examine how fluctuations and modes evolve as the geometry of the condensate is transformed from pancake to toroid. In further calculations, and numerical evaluations the spatial and temporal variables are scaled as  $x/a_{\text{osc}}$ ,  $y/a_{\text{osc}}$  and  $\omega_x t$  respectively, where  $a_{\text{osc}} = \sqrt{\hbar/m\omega_x}$ .

### 2.1. Hartree-Fock-Bogoliubov-Popov formalism

We employ HFB-Popov approximation [29–37] to examine the properties of the collective excitations at  $T = 0$ , and impact of  $U_0$  on the variation in the density distribution at  $T \neq 0$ . In this formalism, the Bose field operator  $\hat{\Psi}$  is decomposed into two parts; the  $c$ -field or the condensate part represented by  $\phi(x, y, t)$  and the non-condensate or the fluctuation part denoted by  $\tilde{\psi}(x, y, t)$ . With  $\hat{\Psi} = \phi + \tilde{\psi}$ , in the mean-field domain the generalized GP equation with the time-independent HFB-Popov approximation is

$$\hat{h}\phi + U[n_c + 2\tilde{n}]\phi = 0, \quad (2)$$

where,  $\hat{h} = (-\hbar^2/2m)(\partial^2/\partial x^2 + \partial^2/\partial y^2) + V(x, y) - \mu$  represents the single-particle part of the Hamiltonian;  $n_c(x, y) \equiv |\phi(x, y)|^2$ ,  $\tilde{n}(x, y) \equiv \langle \tilde{\psi}^\dagger(x, y, t)\tilde{\psi}(x, y, t) \rangle$ , and  $n(x, y) = n_c(x, y) + \tilde{n}(x, y)$  are the local condensate, non-condensate, and total density, respectively. Applying Bogoliubov transformation,  $\tilde{\psi}(x, y, t)$  in terms of quasiparticle modes is

$$\tilde{\psi} = \sum_j \left[ u_j(x, y) \hat{\alpha}_j(x, y) e^{-iE_j t/\hbar} - v_j^*(x, y) \hat{\alpha}_j^\dagger(x, y) e^{iE_j t/\hbar} \right]. \quad (3)$$

Here,  $\hat{\alpha}_j$  ( $\hat{\alpha}_j^\dagger$ ) are the quasiparticle annihilation (creation) operators and satisfy the usual Bose commutation relations, and the subscript  $j$  represents the energy eigenvalue index. The functions  $u_j$  and  $v_j$  are the Bogoliubov quasiparticle amplitudes corresponding to the  $j$ th energy eigenstate. Using the above ansatz and definitions we arrive at the following Bogoliubov-de Gennes (BdG) equations

$$\begin{aligned} (\hat{h} + 2Un)u_j - U\phi^2 v_j &= E_j u_j, \\ -(\hat{h} + 2Un)v_j + U\phi^{*2} u_j &= E_j v_j. \end{aligned} \quad (4)$$

The thermal or non-condensate density  $\tilde{n}$  at temperature  $T$  is

$$\tilde{n} = \sum_j \{ [|u_j|^2 + |v_j|^2] N_0(E_j) + |v_j|^2 \}, \quad (5)$$

where,  $\langle \hat{\alpha}_j^\dagger \hat{\alpha}_j \rangle = (e^{\beta E_j} - 1)^{-1} \equiv N_0(E_j)$  with  $\beta = 1/k_B T$ , is the Bose factor of the  $j$ th quasiparticle state with energy  $E_j$  at temperature  $T$ . However, it should be emphasized that, when  $T \rightarrow 0$ ,  $N_0(E_j)$ 's in Equation (5) vanish. The non-condensate density is then reduced to  $\tilde{n} = \sum_j |v_j|^2$  which represent quantum fluctuations.

It must be mentioned here that the HFB-Popov approximation is gapless, and satisfies Hugenholtz-Pines theorem [38]. Using the theory it is possible to calculate the quasiparticle excitations, and obtain the equilibrium density profiles of the condensate and the thermal densities. The essence of the HFB-Popov theory is to obtain stationary states as self-consistent solutions of Equations (2) and (4). However, the omission of the anomalous average, which accounts for the transfer of particles between condensate and non-condensate clouds, in this theory leads to non-conservation of particle number. This is in contrast to number-conserving theories where the increase in the number of condensate particles should imply a decrease in the number of non-condensate particles. In the present work, through normalization, we maintain constant number of particles, and this translates to a change in the chemical potential.

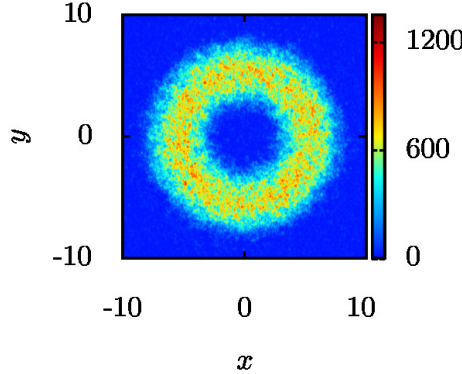


**Figure 1.** (Color online) Equilibrium density profile of the  $^{23}\text{Na}$  condensate at  $T = 20$  nK with  $\sim 10^5$  atoms in a toroidal trap having  $U_0 = 45\hbar\omega_\perp$ , where  $\omega_\perp = 2\pi \times 20$  Hz and  $\lambda = 39.5$ . This has been computed using the SGP method. Density is measured in units of  $a_{\text{osc}}^{-2}$ .

## 2.2. Stochastic Gross-Pitaevskii equation (SGPE)

The time-dependent HFB-Popov theory is well suited to study the quasiparticle modes, and the quantum and thermal fluctuations at equilibrium. It is, however, not suitable to the study the dynamics of condensates [39]. The SGPE, on the other hand, provides a good description of the dynamical evolution of the condensate, and non-condensate clouds. In fact, the experimental realizations have close correspondence to the SGPE results, where the individual results obtained with independent noise realizations are representatives of independent experimental observations. Hence, as one may expect, the experimental results for a system at equilibrium are equivalent to the ensemble average of results from SGPE [40–42]. For the present work we employ SGPE to examine the realistic density distribution of the condensate and non-condensate clouds.

This provides an analysis of the thermal fluctuations sans the knowledge of quasi particle spectrum, and a comparison with the HFB-Popov results has the potential to understand the effects of fluctuations. In the present work we use a scheme based on solving the stochastic Langevin equation for BEC [43] in toroidal traps, and the SGPE is [42]

$$i\hbar \frac{\partial \Psi(\mathbf{x}, t)}{\partial t} = (1-i\gamma) \left[ -\frac{\hbar^2 \nabla^2}{2m} + V_{\text{net}} + U|\Psi(\mathbf{x}, t)|^2 - \mu \right] \Psi(\mathbf{x}, t) + \eta(\mathbf{x}, t). \quad (6)$$

The constant  $\gamma$  denotes the dissipation, and  $\mu$  is the chemical potential. Following the fluctuation-dissipation theorem required for equilibration, the random fluctuation  $\eta(\mathbf{x}, t)$  satisfies the following noise-noise correlation

$$\langle \eta(\mathbf{x}, t) \eta^*(\mathbf{x}', t') \rangle = 2\gamma k_B T \hbar \delta(\mathbf{x} - \mathbf{x}') \delta(t - t'), \quad (7)$$

where  $k_B$  and  $T$  are the Boltzmann constant and temperature respectively, and  $\langle \dots \rangle$  denotes the ensemble average, where each member represents realizations with difference arising from fluctuations. The essence of SGPE is to divide the system into two parts. In which a few highly occupied low-energy quasiparticles are subsumed in the Langevin field  $\Psi(\mathbf{x}, t)$ , and the other part represents a heat bath denoted by the noise term  $\eta$ . The latter also takes incorporate the effects of the higher energy quasiparticles. Another description of the Langevin field is, it is the expectation of the field operator  $\hat{\Psi}$  at zero temperature, and at finite temperatures has contributions from the thermal fluctuations.

In the SGP formalism, the physical properties are computed as an ensemble average over several independent noise realizations, and the total number of atoms at equilibrium is fixed by the chemical potential  $\mu$  irrespective of the change in temperature [44]. As an example the density profile or  $|\Psi(\mathbf{x}, t)|^2$  of one realization is shown in Fig. 1. From the density, at equilibrium, the quasicondensate density  $n_{\text{qc}}(x)$  is extracted through the second order correlation [45–47] as

$$n_{\text{qc}}(x) = n(x) \sqrt{2 - g^{(2)}(x)}, \quad (8)$$

where  $n(x) = |\Psi(x)|^2$ , and  $g^{(2)}(x) = \langle |\Psi(x)|^4 \rangle / \langle |\Psi(x)|^2 \rangle^2$  is the second order correlation function. Thus the quantity  $n(x) - n_{\text{qc}}(x)$  gives us the non-condensate or the thermal density. Pertinent to the present work and as mentioned earlier, thermal fluctuations in toroidal potentials have a direct bearing on the KZ mechanism as discussed in Refs. [48, 49]. These previous theoretical investigations, however, regard the toroidal systems as quasi-1D. In the present work we examine the validity of this assumption in the context of finite temperatures effects, and the observations based on the results from HFB-Popov and SGP theories are given in the next section.

### 3. Results and Discussions

To examine the quasiparticle spectrum with our theoretical scheme, we take BEC of atomic  $^{23}\text{Na}$ , with scattering length  $a = 53.3a_0$  [50, 51], as a test case. Here  $a_0$  is the Bohr radius. The evolution of the quasiparticle modes with the variation of  $U_0$  is computed for  $N_{\text{Na}} = 2 \times 10^3$  with  $\lambda = 39.5$ , and  $\omega_x = \omega_y = \omega_{\perp} = 2\pi \times 20.0$  Hz. The

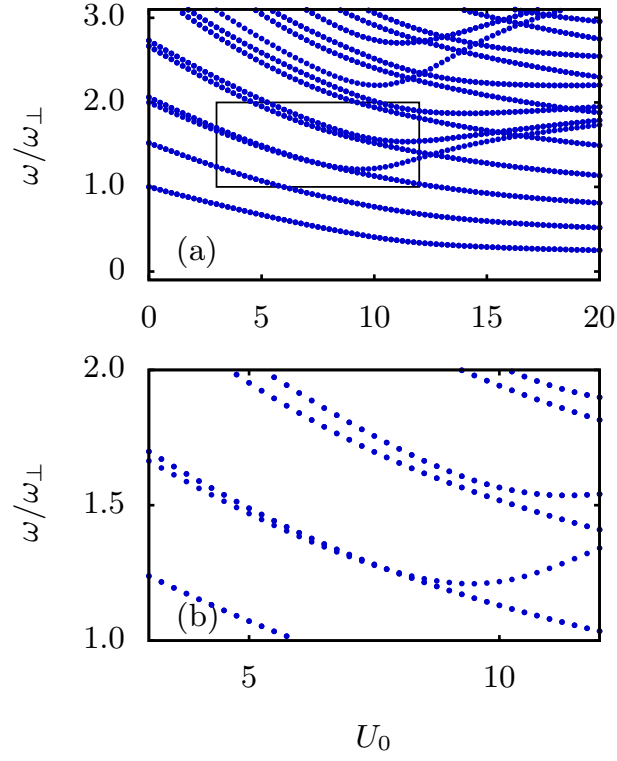


**Figure 2.** (Color online) The evolution of the mode energies as a function of  $U_0$  for  $\alpha = 1$  at  $T = 0$ . (a) Shows the evolution of the low-lying mode energies in the domain  $0 \leq U_0 \leq 20\hbar\omega_\perp$  for  $N_{\text{Na}} = 2 \times 10^3$ . (b) The enlarged view of the region enclosed within the black rectangular box in (a) to resolve the actual level-crossing and quasidegeneracy of modes.

evolution of the low-lying mode energies are shown in Figure 2 as a function of  $U_0$ . It is evident, from the trends in the plot, there are several transformations or changes in the nature of the modes as the condensate is modified from pancake to toroidal geometry.

### 3.1. Decrease in Kohn mode energy

In the absence of the Gaussian potential or when  $U_0 = 0$ , the profile of  $n_c$  has rotational symmetry with the maximum located at the origin, and decreases to zero with  $r > 0$ . The corresponding quasiparticle spectrum has a Goldstone mode, and doubly degenerate Kohn modes with  $\omega/\omega_\perp = 1$ . The quasiparticle amplitudes corresponding to one of the degenerate Kohn modes is shown in Figure 3(a). For  $U_0 \neq 0$ ,  $n_c$  shows a dip in the central region, and an overall increase in the radial extent due to the repulsive Gaussian potential. As  $U_0$  is increased when  $U_0 \approx \mu$ , which occurs when  $U_0 \approx 15\hbar\omega_\perp$ , the condensate cloud is toroidal in shape and hence  $n_c(0,0) \rightarrow 0$ . The change in the geometry, pancake to toroidal, of the  $n_c$  modifies the excitation spectrum and the structure of the Bogoliubov quasiparticle amplitudes. An important observation associated with the change is, the wavelength of excitations becomes longer as they now lie along the circumference of the toroid. This decreases the quasiparticle energies, and



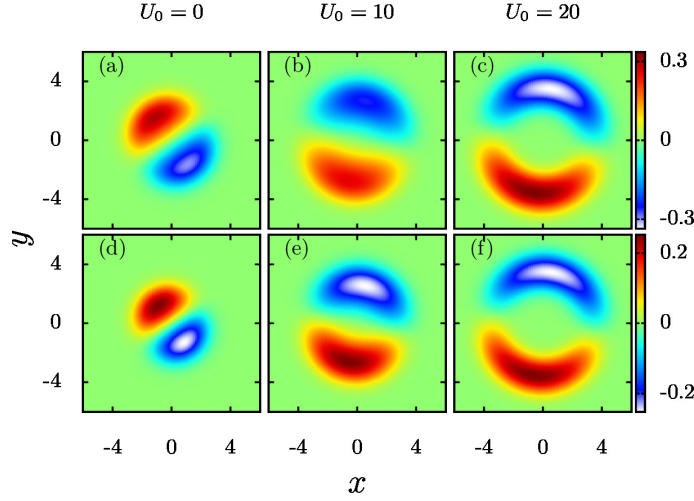


**Figure 3.** (Color online) Evolution of quasiparticle amplitudes corresponding to the Kohn mode as  $U_0$  is increased from 0 to  $20\hbar\omega_\perp$  for  $\alpha = 1$ . (a) - (c) Show the  $u_{\text{Na}}$  corresponding to  $U_0 = 0, 10, 20\hbar\omega_\perp$ , respectively. Harmonic trapping potential is applicable when  $U_0 = 0$ , otherwise, it is a Mexican hat potential. At  $U_0 = 20\hbar\omega_\perp$ , a toroidal shaped BEC is formed and the Kohn modes get deformed. (d) - (f) Show the  $v_{\text{Na}}$  corresponding to  $U_0 = 0, 10, 20\hbar\omega_\perp$ , respectively. In the plots  $u$  and  $v$  are in units of  $a_{\text{osc}}^{-1}$ . Here  $x$  and  $y$  are measured in units of  $a_{\text{osc}}$ .

the evolution of mode energies as a function of  $U_0$  is shown in Figure 2. From the figure, the Kohn mode getting soft with increase in  $U_0$  is discernible. The metamorphosis of the Kohn mode amplitude from pancake to toroidal geometry of the BEC is shown in Figure 3. From the mode functions the ratio of the Kohn mode wavelength at  $U_0 = 20\hbar\omega_\perp$  and  $U_0 = 0$  is  $\approx 4.0$ , which is close to  $\pi$ , the ratio between the diameter and circumference of a circle. It deserves to be mentioned here that for  $15\hbar\omega_\perp < U_0 < 20\hbar\omega_\perp$ , the energy of the Kohn mode gets saturated. This is because the variation in the circumference of the condensate is small, and the change in the wavelength of excitations is negligible.

One distinct trend in the evolution of selected neighbouring mode energy pairs is discernible from the figure. As an example, consider the evolution of breathing and hexapole modes with  $\omega/\omega_\perp = 2.00$ , and  $2.06$ , respectively, at  $U_0 = 0$ . As  $U_0$  is increased, in the domain  $0 < U_0 < 7.5\hbar\omega_\perp$  energies of these two modes are lowered with decreasing separation. At  $U_0 \approx 7.5\hbar\omega_\perp$  the two modes cross over, and when  $U_0 > 7.5\hbar\omega_\perp$  the breathing mode energy increases, however, the hexapole mode energy continues to decrease. The reason behind the increase in breathing mode energy is because it is a  $l = 0$  mode it remains a radial excitation. So, when  $U_0 > 7.5\hbar\omega_\perp$  as the trapping potential assumes toroidal geometry, the effective radial frequency is  $\approx 1.63\omega_\perp$ . The hexapole mode, which has  $l = 3$  is transformed to one along axis of the toroid, and hence, decreases in energy. Similar trend occurs in other neighbouring pairs of states with  $l = 0$ , and the other with  $l > 0$ . It is to be mentioned that, the modes cross over. These crossing are not avoided because  $l$  is a good quantum number, and quasiparticles



with different  $l$  do not mix.

### 3.2. Quantum and thermal fluctuations

At zero temperature the quantum fluctuations, which depend on the  $|v|^2$  of the quasiparticle amplitudes, produce finite  $\tilde{n}$ . Upon closer inspection, we find that the dominant contribution to the number of non-condensate atoms  $\tilde{N} = \int \tilde{n}(x, y) dx dy$  arises from the doubly degenerate Kohn mode. With the variation of  $U_0$ , there is an enhancement of  $\tilde{n}$  as  $U_0$  is increased. There are two reasons behind this, and both are associated with the transition of  $n_c$  from pancake to toroidal structure. First, the Kohn mode energy is lowered, and second, the extrema of the mode functions coincide with the density maxima of  $n_c$ .

For  $T \neq 0$ , the Bose factor  $N_0 \neq 0$ , so in addition to the quantum fluctuations  $\tilde{n}$  have contributions from the thermal fluctuations as well. The latter, however, are orders of magnitude larger in the temperature domain of experimental interest  $\approx 10$  nK. Albeit we have done computations for different temperatures, for the aforementioned reason, we examine the HFB-Popov results for  $T = 10$  nK. The higher  $\tilde{n}$  at finite temperature enhances the interaction between the condensate and non-condensate atoms, represented by the  $\tilde{n}\phi$  term in Equation (2), and modifies  $n_c$ . Due to the repulsive inter-atomic interactions the profile of  $\tilde{n}$  develops a dip in the central region when  $U_0 = 0$ , where the maximum of  $n_c$  is located. In general, as evident from the density plots in Figure 4, due to higher energy the spatial extent of the thermal cloud is larger than the condensate cloud. With higher  $U_0$ ,  $n_c$  develops a dip at the center, and as mentioned in the previous

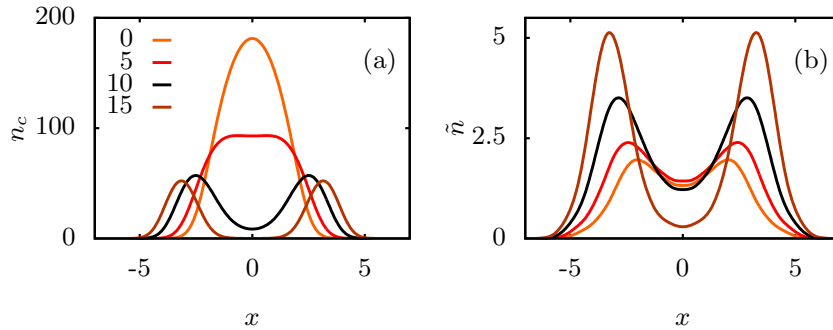


**Figure 4.** (Color online) The plots along  $x$ -axis at  $y = 0$  showing the variation in (a) condensate and (b) non-condensate density profiles at  $T = 10$  nK for different values of  $U_0$ . In the plots  $n_c$  and  $\tilde{n}$  are in units of  $a_{\text{osc}}^{-2}$ . Here  $x$  and  $U_0$  are measured in units of  $a_{\text{osc}}$  and  $\hbar\omega_{\perp}$ , respectively.

section, is transformed to a toroidal condensate when  $U_0 \approx 15\hbar\omega_{\perp}$ . The transformation is evident from the density plots of  $n_c$  as shown in Figure 5. As  $n_c$  and  $\tilde{n}$  are coupled, the density structure of  $\tilde{n}$  is also altered. At  $U_0 = 15\hbar\omega_{\perp}$ ,  $n_c(0, 0) \approx 0.0$  where as  $\tilde{n}(0, 0)$  is still  $\approx 6\%$  of the maximum value. This difference is due to lower  $n_c$  in the central region, and higher energy of the non-condensate atoms. The progressive depletion of  $n_c$  from the central region with higher  $U_0$ , and the corresponding changes in  $\tilde{n}$  are prominent

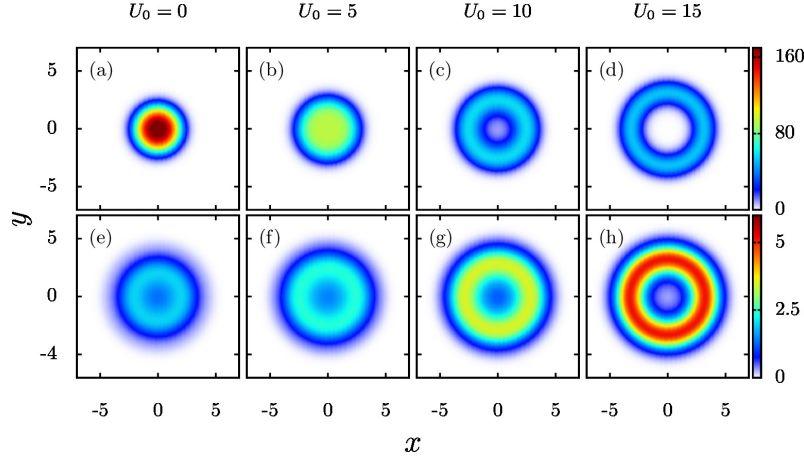


**Figure 5.** (Color online) Condensate and non-condensate density plots at  $T = 10$  nK for different values of  $U_0$ . (a) - (d) plots of condensate, and (e) - (h) non-condensate density distribution for  $U_0 = 0, 5, 10, 15\hbar\omega_\perp$ , respectively. Here  $x$  and  $y$  are measured in units of  $a_{\text{osc}}$ .

in Figure 5 (d), (h). At lower amplitude of the Gaussian potential,  $U_0 < 15\hbar\omega_\perp$ , the maxima of  $n_c$  and  $\tilde{n}$  do not coincide and the separation is  $\approx 2.0a_{\text{osc}}$ . However, when  $U_0 = 15\hbar\omega_\perp$  the separation between maxima is reduced to  $\approx 0.1a_{\text{osc}}$ , the trend in the shifting of the maxima is shown in Figure 4 through the plot of densities along the  $x$ -axis. The number of thermal atoms increases  $\approx 2.5$  fold with increasing the strength of  $U_0$  from 0 to  $15\hbar\omega_\perp$ .

### 3.3. KZ scaling and fluctuations

The KZ mechanism has been the subject of intense investigations in toroidal or multiply connected condensates [48, 49, 52]. One key simplifying assumption in all the works is the consideration of a toroidal condensate as a 1D system with periodic boundary condition. A natural outcome of this assumption is, at finite temperatures the maxima of the condensate and non-condensate densities must lie along the axis of the toroid. Hence, the KZ scaling laws obtained in the previous works [48, 49, 52] are applicable in toroidal condensates only when the parameters of the toroid satisfies the conditions  $\mu \ll U_0$ , and this is an additional criterion to ensure the alignment of the thermal fluctuations. Otherwise, as observed in the present results, the non-condensate or fluctuations distribution have a different geometry, and the system deviates from the 1D approximation. This is an important finding which can only be obtained from finite temperature theories.

## 4. Conclusions

There is a decrease in the Kohn and other mode energies at  $T = 0$  as the external trapping potential is changed from harmonic to a toroidal trapping potential. However,

the trend is not general; close to the pancake to toroidal condensate transition, energies of all the modes with  $l = 0$  increase. Our results provide an understanding on why the nature of fluctuations in toroidal condensates are different from the usual harmonic potential trap. Apart from this, in toroidal traps, the breathing and the hexapole mode contribute to a distinct deviation in the nature of fluctuations from the harmonic trapping potential. This change is evident for  $T = 10\text{nK}$ , when the condensate and thermal densities tend to coincide in toroidal traps. Most important, for the form of the potential considered, combination of a Gaussian and harmonic trapping potentials, the criterion  $\mu \ll U_0$  is a necessary condition to treat the toroidal potential as quasi-1D. This condition highlights the different domains in the geometries of thermal fluctuations in toroidal condensates, and hence, the KZ scaling is applicable only when this criterion is satisfied. Otherwise, the simplifying assumption of quasi-1D geometry for toroidal condensates is not applicable.

## Acknowledgments

We thank K. Suthar, S. Bandyopadhyay and R. Bai for useful discussions. We acknowledge valuable discussions with S. Gautam on SGP method. We also thank the anonymous referees for their thorough review and valuable comments, which contributed to improving the quality of the manuscript. The results presented in the paper are based on the computations using Vikram-100, the 100TFLOP HPC Cluster at Physical Research Laboratory, Ahmedabad, India.

## References

- [1] Kibble T W B 1976 *J. Phys. A* **9** 1387
- [2] Zurek W H 1985 *Nature (London)* **317** 505
- [3] Heathcote W H, Nugent E, Sheard B T and Foot C J 2008 *New J. Phys.* **10** 043012
- [4] Ramanathan A, Wright K C, Muniz S R, Zelan M, Hill W T, Lobb C J, Helmerson K, Phillips W D and Campbell G K 2011 *Phys. Rev. Lett.* **106** 130401
- [5] Moulder S, Beattie S, Smith R P, Tammuz N and Hadzibabic Z 2012 *Phys. Rev. A* **86** 013629
- [6] Marti G E, Olf R and Stamper-Kurn D M 2015 *Phys. Rev. A* **91** 013602
- [7] Hohenberg P and Martin P 1965 *Annals of Physics* **34** 291
- [8] Mermin N D and Wagner H 1966 *Phys. Rev. Lett.* **17** 1133
- [9] Hohenberg P C 1967 *Phys. Rev.* **158** 383
- [10] Berezinskii V L 1972 *Sov. Phys. JETP* **34** 610
- [11] Kosterlitz J M and Thouless D J 1972 *Journal of Physics C: Solid State Physics* **5** L124
- [12] Kosterlitz J M and Thouless D J 1973 *Journal of Physics C: Solid State Physics* **6** 1181

- [13] Stock S, Hadzibabic Z, Battelier B, Cheneau M and Dalibard J 2005 *Phys. Rev. Lett.* **95** 190403
- [14] Hadzibabic Z, Kruger P, Cheneau M, Battelier B and Dalibard J 2006 *Nature (London)* **441** 1118
- [15] Schweikhard V, Tung S and Cornell E A 2007 *Phys. Rev. Lett.* **99** 030401
- [16] Cladé P, Ryu C, Ramanathan A, Helmerson K and Phillips W D 2009 *Phys. Rev. Lett.* **102** 170401
- [17] Tung S, Lamporesi G, Lobser D, Xia L and Cornell E A 2010 *Phys. Rev. Lett.* **105** 230408
- [18] Hung C L, Zhang X, Gemelke N and Chin C 2011 *Nature (London)* **470** 236
- [19] Yefsah T, Desbuquois R, Chomaz L, Günter K J and Dalibard J 2011 *Phys. Rev. Lett.* **107** 130401
- [20] Raman C, Köhl M, Onofrio R, Durfee D S, Kuklewicz C E, Hadzibabic Z and Ketterle W 1999 *Phys. Rev. Lett.* **83** 2502
- [21] Onofrio R, Raman C, Vogels J M, Abo-Shaeer J R, Chikkatur A P and Ketterle W 2000 *Phys. Rev. Lett.* **85** 2228
- [22] Engels P and Atherton C 2007 *Phys. Rev. Lett.* **99** 160405
- [23] Neely T W, Samson E C, Bradley A S, Davis M J and Anderson B P 2010 *Phys. Rev. Lett.* **104** 160401
- [24] Wright K C, Blakestad R B, Lobb C J, Phillips W D and Campbell G K 2013 *Phys. Rev. A* **88** 063633
- [25] Ryu C, Andersen M F, Cladé P, Natarajan V, Helmerson K and Phillips W D 2007 *Phys. Rev. Lett.* **99** 260401
- [26] Wright E M, Arlt J and Dholakia K 2000 *Phys. Rev. A* **63** 013608
- [27] Courtial J, Dholakia K, Allen L and Padgett M J 1997 *Phys. Rev. A* **56** 4193
- [28] Curtis J E and Grier D G 2003 *Phys. Rev. Lett.* **90** 133901
- [29] Griffin A 1996 *Phys. Rev. B* **53** 9341
- [30] Gies C, van Zyl B P, Morgan S A and Hutchinson D A W 2004 *Phys. Rev. A* **69** 023616
- [31] Gies C and Hutchinson D A W 2004 *Phys. Rev. A* **70** 043606
- [32] Gies C 2004 *Hartree-Fock-Bogoliubov treatment of the two-dimensional trapped Bose gas* Master's thesis University of Otago, Dunedin, New Zealand
- [33] Gies C, Lee M D and Hutchinson D A W 2005 *J. Phys. B* **38** 1797
- [34] Roy A, Gautam S and Angom D 2014 *Phys. Rev. A* **89** 013617
- [35] Roy A and Angom D 2014 *Phys. Rev. A* **90** 023612
- [36] Roy A, Gautam S and Angom D 2015 *Eur. Phys. J. Sp. Topics* **224** 571
- [37] Roy A and Angom D 2015 *Phys. Rev. A* **92** 011601(R)
- [38] Hugenholtz N M and Pines D 1959 *Phys. Rev.* **116** 489

- [39] Wild B G 2011 *The Hartree-Fock-Bogoliubov Theory of Bose-Einstein Condensates* Ph.D. thesis University of Otago, Dunedin, New Zealand
- [40] Cockburn S and Proukakis N 2009 *Laser Physics* **19** 558
- [41] Gautam S, Roy A and Mukerjee S 2014 *Phys. Rev. A* **89** 013612
- [42] Cockburn S P and Proukakis N P 2012 *Phys. Rev. A* **86** 033610
- [43] Ford G W, Lewis J T and O'Connell R F 1988 *Phys. Rev. A* **37** 4419
- [44] Shukla V, Brachet M and Pandit R 2013 *New J. Phys.* **15** 113025
- [45] Prokof'ev N, Ruebenacker O and Svistunov B 2001 *Phys. Rev. Lett.* **87** 270402
- [46] Cockburn S P, Negretti A, Proukakis N P and Henkel C 2011 *Phys. Rev. A* **83** 043619
- [47] Proukakis N P 2006 *Phys. Rev. A* **74** 053617
- [48] Das A, Sabbatini J and Zurek W H 2012 *Scientific Reports* **2** 352
- [49] Weiler C N, Neely T W, Scherer D R, Bradley A S, Davis M J and Anderson B P 2008 *Nature* **455** 948
- [50] Davis K B, Mewes M O, Andrews M R, van Druten N J, Durfee D S, Kurn D M and Ketterle W 1995 *Phys. Rev. Lett.* **75** 3969
- [51] Stamper-Kurn D M, Andrews M R, Chikkatur A P, Inouye S, Miesner H J, Stenger J and Ketterle W 1998 *Phys. Rev. Lett.* **80** 2027
- [52] Su S W, Gou S C, Bradley A, Fialko O and Brand J 2013 *Phys. Rev. Lett.* **110** 215302